Pattern orientation due to longitudinal fields in a cavity with Kerr media

Daniel A. Mártin

Departamento de Física, Facultad de Ciencias Exactas y Naturales, Universidad Nacional de Mar del Plata and Instituto de Investigaciones Físicas de Mar del Plata (Consejo Nacional de Investigaciones Científicas y Técnicas), Funes 3350, 7600 Mar del Plata, Argentina

(Received 7 November 2012; published 23 August 2013)

When describing field propagation in a ring cavity, longitudinal fields are usually neglected. Although small, the longitudinal component is always present in finite width beams. An equation describing field propagation in Kerr media and inside a ring cavity filled with such medium is derived. Coupling among longitudinal and transverse fields but also other usually neglected terms are considered. Numerical integration results show that coupling with longitudinal field can orientate the resulting pattern along the polarization direction.

DOI: 10.1103/PhysRevA.88.023843 PACS number(s): 42.65.Sf, 05.45.−a

I. INTRODUCTION

Pattern formation in nonlinear media has been widely studied from the theoretical and numerical point of view [1]. A usually studied model consists of a ring cavity filled with Kerr media [2], subject to linearly polarized plane incoming fields. This system, in the mean-field approximation, can be described by the Lugiato-Lefever equation [3].

When analyzing pattern formation, translational but also rotational symmetry are expected. It is usually assumed that the system does not have a preferred direction, and a spontaneous pattern formation, with random orientation, breaks that symmetry. In optical systems, hexagonal patterns are usually found.

Physical fields have a finite width; thus translational symmetry is broken in experiments. Also, since the divergence of the displacement should be zero for materials with no free charges, there has to be a small, usually neglected, longitudinal field. Nonlinear polarization couples this field to transverse field [4], in a way similar to what happens for elliptically polarized fields in Kerr media [5]. As we shall see, this coupling may break rotational symmetry of the system.

There are some numerical results for Gaussian beams in Kerr media, but there are very few studies about longitudinal fields in nonlinear media. In [6], propagation equations are derived, and in [7] filamentation is studied. In all such cases beam waist is assumed to be small, which results in relatively large longitudinal fields. Here, we are interested in pattern forming systems, where broad beam waists and small longitudinal fields are expected.

The purpose of this paper is to numerically study whether broken symmetries may affect pattern formation in a ring cavity and to what extent results derived for plane waves are valid when finite beam widths are considered.

The article is organized as follows. In Sec. II, we introduce the problem under study. In Sec. III, we comment on results for linear media. In Sec. IV, we outline the derivation of an evolution equation in Kerr media, taking into account longitudinal fields; in Sec. V, we introduce an equation describing field propagation in a ring cavity; in Sec. VI, we numerically integrate that equation; in Sec. VII, we comment on our results and in Sec. VIII we draw our conclusions. An outline of lengthy calculations is performed in the Appendixes.

II. STATEMENT OF THE PROBLEM

We will assume that a quasimonochromatic electric field $\vec{E}$ propagates in a Kerr medium along the z direction, with no y component. The field can be written as a solution to the linear monochromatic problem multiplied by a slowly varying envelope $\mathcal{E}$:

$$\vec{E} = \vec{\mathcal{E}}(\vec{r},t)e^{i(k_0 z-\omega_0 t)} + \text{c.c.}, \tag{1}$$

where ω_0 is the angular frequency; $k_0 = k(\omega)|_{\omega=\omega_0}$ is the wave number, with $k(\omega) \doteq \frac{\omega}{c}\sqrt{\tilde{\varepsilon}_r(\omega)}$, $\tilde{\varepsilon}_r$ is the relative permittivity, and c is the speed of light in vacuum. Since the divergence of the displacement is zero, there should be a longitudinal field, $\mathcal{E}_z$, which may be approximated by

$$\mathcal{E}_{z,\text{approx}} = \frac{i}{k_0}\partial_x \mathcal{E}_x, \tag{2}$$

where $\partial_q \doteq \frac{\partial}{\partial q}$. If $\mathcal{E}_x$ is a smooth function of $\rho \doteq \sqrt{x^2+y^2}$, whose width is approximately r_0, then an estimate of the longitudinal field amplitude is $|\mathcal{E}_{z,\text{approx}}| \sim (r_0 k_0)^{-1}|\mathcal{E}_x|$.

In pattern forming systems, beam waists tend to be much larger that field wavelength, so that $\mathcal{E}_z$ should be a small quantity. Suppose that $\mathcal{E}_x$ has rotational symmetry, for instance, it has a Gaussian profile, $\mathcal{E}_x = \mathcal{E}_0 e^{-\rho^2/r_0^2}$. Since $\partial_x = (x/\rho)\partial_\rho$, then, $\mathcal{E}_{z,\text{approx}}$ does not have rotational symmetry. Also, for plane incoming fields, when a pattern is formed, there are places in the transverse plane where electric-field intensity is greater than their vicinity, thus, through Eq. (2), longitudinal fields should be formed.

III. RESULTS FOR FINITE WIDTH BEAMS IN LINEAR MEDIA

For a single frequency Gaussian beam in linear medium, solutions to Maxwell equations in terms of a series expansion have already been derived [8–12]. Its first term is $E_x(\vec{r},t) = \mathcal{E}_{\text{parax}}e^{i(k_0 z-\omega t)} + \text{c.c.}$, where $\mathcal{E}_{\text{parax}}$ is the Gaussian beam under paraxial approximation. It is a solution of

$$(2ik_0\partial_z + \nabla_\perp^2)\mathcal{E}_x = 0, \tag{3}$$

with Gaussian shape at $z = 0$. Its explicit form can be found in [13]. The first longitudinal term can be calculated with (2). Higher-order terms are solutions of equations similar to (3) and are zero at $z = 0$.

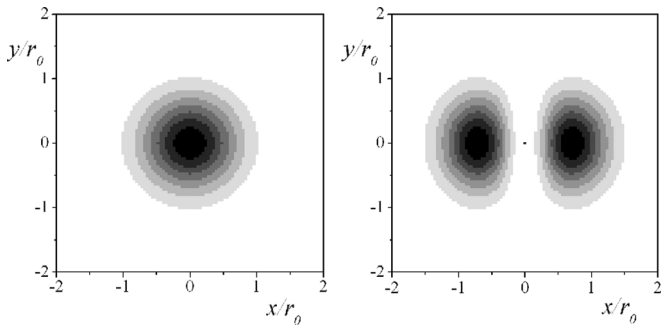

FIG. 1. Intensity of the x and z components of the electric field as a function of the transverse coordinates x/r_0 and y/r_0, for a monochromatic Gaussian beam in a linear medium with $r_0k_0 = 2400\pi$. Results correspond to a distance of $\Delta z = 2000\pi/k_0$ from the least waist plane and were derived using the angular spectrum representation. Left: $|E_x|^2$. Right: $|E_z|^2$. White is used for lower intensities and black is used for higher intensities. The largest intensity of the longitudinal field is about 1.3×10^{-8} times the peak value of transverse field.

For monochromatic fields in linear media, assuming that the field propagates in only one direction, and knowing E_x on the plane $z = 0$, we may calculate E_x exactly in any other place, for instance, by means of the angular spectrum representation. Also, since the divergence of the electric field is zero, we may calculate E_z exactly. The exact solution and series solution have been compared in [8]. It can be seen that the series solution works well for distances up to $z_t = \sqrt{2}k_0^2r_0^3$. Since we will be studying broad waist situations, series solutions should be adequate.

In Fig. 1, we have numerically calculated transverse and longitudinal components of a monochromatic Gaussian field in a linear medium, by means of the angular spectrum representation. It can be seen that the z component of the field does not have rotational symmetry. We have performed similar calculations for super Gaussian fields and found similar results.

If we had considered circular or elliptical polarization, $\mathcal{E}_{z,\text{approx}}$ would have been given by $\mathcal{E}_{z,\text{approx}} = \frac{i}{k_0}(\partial_x\mathcal{E}_x + \partial_y\mathcal{E}_y)$, instead of (2). For instance, for a circularly polarized Gaussian beam, E_z would consist in two lobes like the ones in Fig. 1 rotating at frequency ω_0. Thus no orientational effect would be expected. In the rest of the article we will limit ourselves to the linearly polarized case.

IV. WAVE PROPAGATION IN KERR MEDIA

Starting from Maxwell's equations, it is straightforward to obtain a (nonlinear) wave equation, which can be written as

$$\nabla_\perp^2\vec{E} + \partial_z^2\vec{E} - \boldsymbol{\nabla}(\boldsymbol{\nabla}\cdot\vec{E}) = \mu_0\partial_t^2(\vec{P}_L + \vec{P}_{NL}), \tag{4}$$

where $\nabla_\perp^2$ is the transverse Laplacian, $\nabla_\perp^2 = \partial_x\partial_x + \partial_y\partial_y$; $\vec{P}_L$ is the linear polarization and $\vec{P}_{NL}$ is the nonlinear polarization. In nonlinear media with no free charges, although the divergence of the displacement is zero, the divergence of the electric field is not necessarily zero: Gauss equation can be written as

$$\varepsilon_0\boldsymbol{\nabla}\cdot\vec{E} = -\boldsymbol{\nabla}\cdot(\vec{P}_L + \vec{P}_{NL}). \tag{5}$$

Polarization may be dispersive, and can be properly related to the electric field in the frequency domain, or like convolutions in time domain; see [14, sec. 2d]. Assuming that the medium is isotropic and centrosymmetric, and has a Kerr-like nonlinearity, the ith component of linear polarization may be written as

$$\tilde{P}_{L,i}(\omega) = \varepsilon_0[\tilde{\varepsilon}_r(\omega) - 1]\tilde{E}_i(\omega). \tag{6}$$

Nonlinear polarization may be written as

$$\tilde{P}_{NL,i}(\omega_0) = \frac{\varepsilon_0}{4\pi^2}\iiint\tilde{\chi}^{(3)}_{ijkl}(\omega_1,\omega_2,\omega_3)\tilde{E}_j(\omega_1)\tilde{E}_k(\omega_2)\tilde{E}_l(\omega_3) \times\delta(\omega_0-\omega_1-\omega_2-\omega_3)d\omega_1d\omega_2d\omega_3+\cdots, \tag{7}$$

where summation over repeated indices is assumed. Diverse symmetry relationships greatly reduce the number of independent elements of $\chi^{(3)}_{ijkl}$ to 2 [14]. Under the slowly varying envelope approximation (SVEA), nonlinear polarization can be written as $\vec{P}_{NL} = \vec{\mathcal{P}}_{NL}e^{i(k_0z-\omega_0t)} + \text{c.c.}$, with [14]

$$\mathcal{P}_{NL,x} = 3\varepsilon_0\tilde{\chi}^{(3)}\left[|\mathcal{E}_x|^2\mathcal{E}_x + A_E|\mathcal{E}_z|^2\mathcal{E}_x + \frac{B_E}{2}\mathcal{E}_z^2\overline{\mathcal{E}_x}\right], \tag{8}$$

where $\overline{Q}$ is the complex conjugate of Q; $\tilde{\chi}^{(3)}$ is the Fourier transform of the nonlinear susceptibility $\chi^{(3)}_{xxxx}$, evaluated at $(\omega_0,\omega_0,-\omega_0)$; A_E and B_E are related to the coupling among fields in perpendicular directions, and fulfill the following relation: $A_E + B_E/2 = 1$.

Field evolution may be found solving (4) and (5) with a polarization given by (6) and (7). We propose a solution to those equations like (1), with $|\partial_z\mathcal{E}_{x/z}| \ll k_0\mathcal{E}_{x/z}$ and $|\partial_t\mathcal{E}_{x/z}| \ll \omega_0\mathcal{E}_{x/z}$. Field amplitudes $\mathcal{E}_x$ and $\mathcal{E}_z$ are expressed as series solutions based on the multiple scales analysis [15], where terms and coordinates are organized in powers of a small parameter α. Explicitly, electric field is written as $\vec{\mathcal{E}} = \vec{\mathcal{E}}^{(0)} + \alpha\vec{\mathcal{E}}^{(1)} + \alpha^2\vec{\mathcal{E}}^{(2)} + \cdots$, and depends on slow coordinates, $X_i = \alpha^i x$, $Y_i = \alpha^i y$, $Z_i = \alpha^i z$, and $T_i = \alpha^i t$, where $i \geqslant 1$.

In order to find an equation which, after neglecting nonlinear terms and dispersion, reduces to (3), we assume that the transverse Laplacian, the z and time derivatives over $\mathcal{E}_x$, and the most relevant nonlinear terms in (4) are of order α^2. This condition is achieved if fields do not depend on Z_1 nor T_1.

Evolution equations are found solving (4) and (5) at each order of α. Up to order α^2, no new terms are included, so the approximation of (4), valid to that order, is (the derivation is commented on in the Appendixes)

$$\frac{\partial\mathcal{E}_x}{\partial z} + k'\frac{\partial\mathcal{E}_x}{\partial t} \simeq \frac{i}{2k_0}\nabla_\perp^2\mathcal{E}_x + \frac{i\omega_0^2}{2k_0c^2}3\tilde{\chi}^{(3)}|\mathcal{E}_x|^2\mathcal{E}_x, \tag{9}$$

with $k' \doteq \partial_\omega[\frac{\omega}{c}\sqrt{\tilde{\varepsilon}_r(\omega)}]|_{\omega=\omega_0}$. This result is the well-known nonlinear Schrödinger equation (NLSE), usually used for describing field propagation in nonlinear media [14].

Longitudinal field couples to the transverse field through nonlinear polarization [see Eq. (8)], and that contribution should be of order α^4. At order α^3, $\boldsymbol{\nabla}\cdot\vec{E} \neq 0$. Thus the approximation (2) is no longer valid, and evolution equations for $\mathcal{E}_x$ and $\mathcal{E}_z$ have to be obtained separately. However, an evolution equation can be found, where $\mathcal{E}_z$ is replaced by functions of $\mathcal{E}_x$; see the Appendixes.

The equivalent to (9), valid to order α^4, is

$$2ik_0(\partial_z + k^{'}\partial_t)\mathcal{E}_x = -\left[\nabla_\perp^2 + \partial_z^2 - (k^{'2} + k_0 k^{''})\partial_t^2\right]\mathcal{E}_x - \omega_0^2\mu_0\mathcal{P}_{NL,x} - 3i\left[2\left(\partial_{\omega_1}k^2_{(3)}|_0\right)\left|\mathcal{E}_x^2\right|\partial_t\mathcal{E}_x + \left(\partial_{\omega_3}k^2_{(3)}|_0\right)\mathcal{E}_x^2\partial_t\overline{\mathcal{E}_x}\right]^{(4)} + [\partial_x\nabla\cdot(\vec{\mathcal{E}}e^{i(k_0 z-\omega_0 t)})]^{(4)}, \quad (10)$$

where $[Q]^{(n)}$ is an approximation of Q correct up to order α^n; $k'' \doteq \partial^2_\omega[\frac{\omega}{c}\sqrt{\tilde{\varepsilon}_r(\omega)}]|_{\omega=\omega_0}$; the symbol "$|_0$" means that the derivative of $k^2_{(3)}$ is evaluated at $(\omega_0,\omega_0,-\omega_0)$, and $k_{(3)}$ is the same as in [15]: $k^2_{(3)}(\omega_1,\omega_2,\omega_3) \doteq \frac{k_0^2(\omega_1+\omega_2+\omega_3)\tilde{\chi}^{(3)}_{xxxx}(\omega_1,\omega_2,\omega_3)}{\tilde{\varepsilon}_r(\omega_1+\omega_2+\omega_3)}$.

The second derivative with respect to time in Eq. (10) is related to group-velocity dispersion effects; the second derivative with respect to z is a nonparaxial correction that can be rewritten in an easier way. The term $\mathcal{P}_{NL,x}$ accounts for the usually considered nonlinear term but also includes the symmetry breaking coupling to the longitudinal field [see Eq. (8)]. The following term includes small functions related to frequency dispersion effects acting on nonlinear terms (see Appendixes). The last term in Eq. (10) comes from the nonvanishing electric-field divergence. It includes another nonsymmetric contribution and can be calculated straightforward from (5); see Appendixes.

In order to obtain an equation useful for numerical computation, we may perform a change of variables towards coordinates traveling with the wave: $\xi = z$, $\tau = t + k'z$. We also need to get rid of z (or ξ) first and second derivatives on the right side of Eq. (10). This can be achieved using Eq. (9), which is valid to order α^2, and the z derivative of that equation, repeatedly (see Appendixes). Finally, we get

$$\partial_\xi\mathcal{E}_x = \frac{i}{2k_0}\nabla_\perp^2\mathcal{E}_x + \frac{i\omega_0^2}{2k_0c^2}3\tilde{\chi}^{(3)}|\mathcal{E}_x|^2\mathcal{E}_x - i\frac{k''}{2}\partial_\tau^2\mathcal{E}_x + i(N_N + N_L + N_T). \quad (11)$$

Expressions for new terms (N_N, N_L, and N_T) can be found in the Appendixes.

Terms that should break rotational symmetry, related to the coupling with longitudinal field and $\nabla\cdot\vec{E}$ (which is equal to $-\nabla\cdot\vec{P}_{NL}/[\varepsilon_0\tilde{\varepsilon}_r(\omega_0)]$), are included in $\hat{N}_N$. Simple inspection shows that asymmetric terms contribute to (i.e., have the same sign as) the nonlinear polarization, and are aligned to the field polarization. However, their effect is rather small.

Terms like $\partial_\tau\mathcal{E}_x$ and $-\nabla_\perp^2\mathcal{E}_x$ are included in $\hat{N}_L$: they have rotational symmetry if $\mathcal{E}_x$ has that symmetry, but become asymmetric for asymmetric fields. Their asymmetric part should contribute to the expected orientation effect.

Time derivatives of nonlinear terms are included in $\hat{N}_T$. They are related to dispersive effects and are similar to the ones derived for ultrashort plane-wave pulses [16]. Here we are interested in short linewidth pulses and thus dispersive effects should be small. Fifth- or higher-order nonlinear effects are neglected.

An expression similar to Eq. (10) was derived in [7], where beam filamentation was studied in a semi-infinite medium. There, single frequency fields were studied; thus no time derivatives were considered.

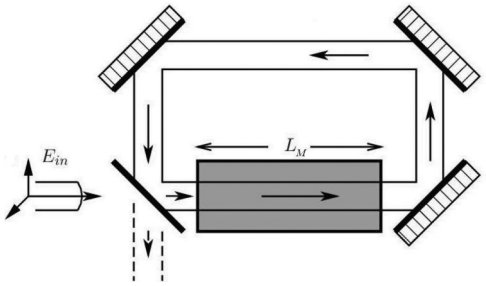

FIG. 2. Ring cavity scheme.

V. FIELD PROPAGATION IN THE CAVITY

We study a system like the one described in Fig. 2. It consists of a ring cavity filled with a Kerr medium. The input field has amplitude $E_{\rm in}$, the entrance mirror is partly transparent, with reflection coefficient r_i (which is assumed to be close to 1) and transmission coefficient t_i. All other mirrors are perfect. Nonlinear material and surrounding media have the same refractive index. Round-trip length is L, the round-trip detuning is θ, and round-trip time is $\tau_r = k'L_M + k'_S(L - L_M)$, where $L_M \leqslant L$ is the nonlinear material length and k'_S is the inverse of group velocity in the surrounding medium.

We take into account wave propagation both in the nonlinear and the linear medium, of length $L - L_M$. For the sake of simplicity, we assume that linear medium refractive index and group velocity are the same as in the nonlinear medium (when the field tends to zero), and we neglect group-velocity dispersion in linear media. Applying the classical method for obtaining equations in a ring cavity [15], and normalizing the quantities, we get

$$\frac{\partial A}{\partial t'} = A_{\rm in} - (1 + i\Theta)A + i\nabla_\perp^{'2}A + i\gamma_e|A^2|A - iG\partial_{t'}^2A + \hat{O}, \quad (12)$$

where γ_e is the electric nonlinearity sign (it is 1 for focusing and -1 for defocusing materials), and $\Theta = -\frac{\theta r_i}{(1-r_i)}$.

Fields have been normalized:

$$A = \frac{\mathcal{E}_x}{C}, \quad A_{\rm in} = \frac{t_i}{(1-r_i)}\frac{E_{\rm in}}{C}, \quad (13)$$

where $C = E_c\sqrt{\frac{2\tilde{\varepsilon}_r(\omega_0)(1-r_i)}{3Lk_0r_i}}$, and E_c is a characteristic field amplitude such that $\tilde{\chi}^{(3)}E_c^2 = \gamma_e$. Transverse coordinates and time were normalized, $x' = x/l$, $y' = y/l$, and $t' = t\frac{(1-r_i)}{\tau_r}$, where $l = \sqrt{\frac{Lr_i}{2k_0(1-r_i)}}$.

If $\hat{O}$ were zero, we would recover a broadly used model for pattern formation analysis in passive and active systems [1], and which may also be used for describing other systems like Fabry-Pérot cavities [2]. Within that model, there is no bistability for $\Theta\gamma_e < \sqrt{3}$. Perturbations of the steady homogeneous solution, with transverse wave numbers $\vec{q}$, decay exponentially unless $(\Theta + q^2) > \sqrt{3}$ and $3\gamma_e|A^2| - 2(\Theta + q^2) \geqslant \sqrt{(\Theta + q^2)^2 - 3}$. For instance, for $\gamma_e = 1$ and $\Theta = 1$, the lowest unstable intensity is $|A^2| = 1$, and the critical transverse wave numbers fulfill $|q|^2 = 1$. This means that a set of wave numbers forming a circle in the transverse wave-number space becomes simultaneously unstable. So, there should be no preferred direction for the pattern forming

instability. The circle of unstable wave numbers finally turns into a hexagon with random orientation.

New terms can be written as $\hat{O} = \hat{O}_N + \hat{O}_L + \hat{O}_T$, which are the normalized versions of N_L, N_N, and N_T. An expression for new terms is

$$\begin{aligned}\hat{O}_T &= -[2K_{T1}|A^2|\partial_t A + K_{T2}A^2\partial_t \bar{A}],\\ \hat{O}_N &= iK_N\gamma_e\left[\left(1+\frac{B_E}{2}\right)A^2\partial^2_{x'}\bar{A} + \left(1+\frac{B_E}{2}\right)\right.\\ &\quad\left.\times\ |A|^2\partial^2_{x'}A + (4+B_E)A|\partial_{x'}A|^2 + (\partial_{x'}A)^2\bar{A}\right],\end{aligned} \tag{14}$$

and

$$\begin{aligned}\hat{O}_L = \frac{-iK_N}{4}&[((L/L_M)|A|^2 + \gamma_e\nabla'^2_\perp)|A|^2A\\ &+(2\gamma_e|A|^2 + \nabla'^2_\perp + 2ir_i\partial_{t'})\nabla'^2_\perp A - A^2\nabla^2_\perp\bar{A}]\\ &+\gamma_e K_L\partial_{t'}(|A^2|A),\end{aligned}$$

with constants

$$\begin{aligned}K_L &= \frac{k_0'(1-r_i)}{\tau_r k_0},\quad K_N = \frac{2(1-r_i)}{k_0 r_i L},\\ K_{Ti} &= \frac{\tilde{\varepsilon}_r(\omega_0)(1-r_i)}{\tau_r k_0^2}\partial_{\omega_i}k^2_{(3)}|_0/|\tilde{\chi}^{(3)}|,\end{aligned} \tag{15}$$

and

$$G = \frac{r_i L_M k''(1-r_i)}{2\tau_r^2}. \tag{16}$$

We have neglected losses both in linear and nonlinear medium. It can be shown that small losses may be taken into account and the same equation can be found with a different normalization; see [14].

In order to estimate the values new constants may take, we consider a wave number in the optical region ($k_0 = 2\pi/500$ nm), a semitransparent mirror with $r_i = 0.95$, and a round-trip length of roughly $L = 20$ cm. If the material is away from resonances, from Drude model, we may estimate $k_0' \sim k_0/\omega_0$ and $k_0'' \sim k_0/\omega_0^2$. Having in mind that $L \sim c\tau_r$, it is reasonable to estimate K_N and K_L to be roughly 10^{-6}–10^{-7}. A similar value for G would be correct in cavities filled with a nonlinear medium, and smaller values would be right for partly filled cavities. In order to estimate values for $\partial_{\omega_i}k^2_{(3)}$, we may consider a model for nonlinear effects. For instance, the classical anharmonic-oscillator model [4] is adequate for electronic nonlinearities. Within the model, it is assumed that electrons are placed in symmetric potential wells, whose shape is slightly different from a parabola. Following the derivations in [4], and using previously mentioned values for other constants, we may estimate that K_{T1} and K_{T2} are of the same order as K_L.

We may also estimate $l \simeq 0.4$ mm and $C^2 \simeq \frac{4\tilde{\varepsilon}_r(\omega_0)}{3}\times 10^{-8}E_c^2$, so the refraction index may change in about 10^{-8} due to nonlinear effects.

VI. NUMERICAL INTEGRATION RESULTS

A. General results

Equation (12) was numerically integrated [17], with $\Theta = 1$ and $\gamma_e = 1$. We chose $A_E = B_E = 2/3$, which is the predicted value for electronic nonlinearities [4, p. 211]. We took $G = K_L = L_N = K_{T1} = K_{T2} = 10^{-7}$ unless otherwise stated. A Gaussian incoming field was also proposed:

$$A_{\rm in} = A_{\rm in0}e^{-\rho'^2/\rho_0'^2}. \tag{17}$$

For plane incoming waves ($\rho_0' = \infty$), if we choose $\Theta = 1$ and $\gamma_e = 1$, neglecting terms of order α^3 or higher, it is widely known that there is a critical value $|A_{\rm in0}|^2 \doteq I_{\rm in} = 1$ [in that situation, the steady homogeneous solution corresponds to the already mentioned case $|A|^2 = 1$; see Eq. (12)] [1,3]. Above that value, a hexagonal pattern shows up, whose transverse wavelength is 2π. We have performed numerical integrations for plane incoming fields taking into account terms of order α^4 [Eq. (12)]. We have not found any noticeable difference for the final stage.

For large values of ρ_0' ($\rho_0' > 80$, measured in terms of l), numerical integration results show a hexagonal pattern with no preferential orientation, and wavelength close to 2π. For lower values of ρ_0' (roughly $\rho_0' \leqslant 60$), hexagonal patterns were also found, most of them were oriented like the lobes of $\mathcal{E}_z$. In Fig. 3, numerical integration results are shown for $\rho_0' = 40$. Notice that under the above assumptions, this is a broad waist (roughly 1.5 cm). It can be seen that, if we rotate the coordinate system by an angle φ, then the solution (i.e., the pattern that shows up) also rotates. In order to measure the rotation angle of the pattern, we define φ_P as the complementary of the angle formed by the brightest point in the far field (the far field is related to the Fourier transform of the pattern) and the x axis. We found that φ_P closely matches φ. The same results were found with super Gaussian fields of order 2, $A_{\rm in} = A_{\rm in0}e^{-(\rho'^2/\rho_0'^2)^2}$, with radius $\rho' = 50$.

Other integration results are shown in Fig. 4: for small waists, $\rho_0' = 15$; the pattern shape depends on K_N: for $K_N = 10^{-7}$ a hexagonal pattern, similar to those shown in Figs. 4(b_1) and 4(b_2), is formed, but for $K_N = 10^{-6}$ a different hexagonal pattern is formed [see Figs. 4(a_1) and 4(a_2)]. For some values of ρ_0', for instance, $\rho_0' = 28$, the pattern does not always have the right orientation: notice that in Fig. 4(b_2), the pattern is rotated 90° from expected orientation. Increasing the value of K_N (taking $K_N \geqslant 10^{-4}$), we recover the correct orientation. Finally, for $\rho_0' = 60$, patterns orientate as expected, and it can be seen that the pattern is larger in the direction perpendicular to field polarization; see Figs. 4(c_1) and 4(c_2).

We also found that critical intensity for which pattern shows up increases as ρ_0' decreases. For instance, for $\rho_0' = 15$, an intensity $I_{\rm in} = 1.12$ is needed. Increasing incoming intensity further may cause defects; some of them resemble the pentagons and heptagons in [18].

B. Noise

It may be argued that since longitudinal fields are small, their effects may wash out the orientation effects. Noise in lasers is usually measured in terms of the relative intensity noise (RIN): $\langle\frac{\delta P}{P}\rangle \simeq \sqrt{2\int_{\omega_1}^{\omega_2}S(\omega)d\omega}$, where P is the average power (proportional to the integral of $|A_{\rm in}|^2$ over the transverse surface), δP is the power fluctuation, $\omega_{1,2} > 0$ are the frequencies we are considering, and $S(\omega)$ is the power spectral density (roughly, square of the module of the Fourier transform of the relative power). Ten times the logarithm of $S(\omega)$ may

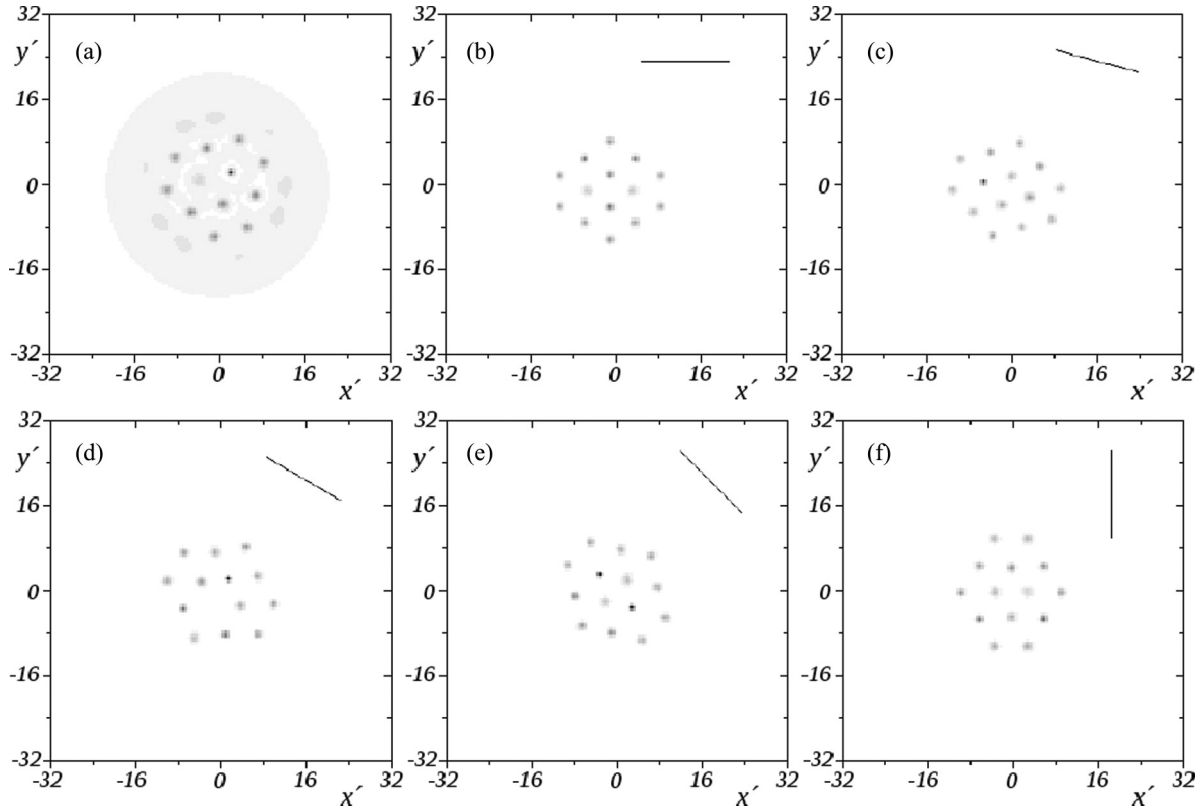

FIG. 3. Patterns formed for $\rho_0 = 40$, $I_{\rm in} = 1.035$, and $t' = 680$. In each window 1/4 of the integration area is shown (notice that x and y range from $-32l$ to $32l$). In (a) terms of order α^4 are neglected. In all other cases, we take $G = K_N = K_L = K_{T1} = K_{T2} = 10^{-7}$. The system is rotated with respect to the integration region by an angle φ, and the angle formed by the pattern, φ_P, is measured. In (b), $\varphi = 0^\circ$ and $\varphi_P = 3^\circ$; in (c), $\varphi = 15^\circ$ and $\varphi_P = 15^\circ 22'$; in (d), $\varphi = 30^\circ$ and $\varphi_P = 27^\circ 37'$; in (e), $\varphi = 45^\circ$ and $\varphi_P = 47^\circ 44'$; in (f), $\varphi = 90^\circ$ and $\varphi_P = 27^\circ$ (which is equivalent, since we are studying regular hexagons, to $\varphi_P = 87^\circ$). A short line showing polarization direction was added to the upper right corner of each window.

take values as low as -160 dB/Hz in low linewidth lasers (100 KHz or less) [19]. If we take $\omega_2 - \omega_1$ of the order of the linewidth, values for $\frac{\delta P}{P}$ as low as 10^{-5}–10^{-6} can be obtanied.

In order to account for input laser noise, we have run numerical simulations of Eq. (12), but now with $A_{\rm in} = A_{\rm in0} e^{-\rho'^2/\rho_0'^2}[1 + f(x,y,t)]$, where $f(x,y,t)$ is a complex—in order to simulate phase inhomogeneities—random distribution with zero mean, bounded by a small number e: $[|{\rm Re}(f)| < e/2$ and $|{\rm Im}(f)| < e/2]$. We used the parameters of Fig. 3(d), and intended to reproduce its results. We calculated the rate of numerical integrations in which the pattern orientates as expected. Based on the results of the previous subsection, we say that the pattern "orientates as expected" if $|\varphi - \varphi_P| < 6^\circ$. Notice that, since we are taking two 6° ranges, and the orientation angle is reduced to the 0°–60° range, if pattern orientation were random, we would find that 1/5 of the simulations orientate as expected; hence, if there is a measurable effect, greater rates should be measured.

First, we ran some simulations with homogeneous noise, i.e., where $f(x',y') = f(0,0)$, We found that five out of five simulations oriented as expected for $e = 10^{-6}$, $10^{-5}, 10^{-4}, 10^{-3}, 10^{-2}$, and $e = 10^{-1}$. In these cases, $\langle \frac{\delta P}{P} \rangle = e$.

We have also considered the most anisotropic noise we could simulate: $f(x,y,t)$ being complex, zero mean, spatially uncorrelated random function. This was numerically achieved defining f as a set of 512×512 complex random numbers, which were chosen in every integration step. Every random number was chosen independently of the rest of them.

For the anisotropic case, we ran eight simulations for each of the following values of e: $e = 10^{-5}$ (found eight cases oriented as expected), $e = 10^{-3}$ (found six cases oriented as expected), $e = 10^{-2.5}$ (found six cases oriented as expected), $e = 10^{-2}$ (found four cases oriented as expected), and $e = 10^{-1.5}$ (found two cases oriented as expected). In this case, since the noise at two different points may have opposite sign, noise was lower. The measured noise was $\langle \frac{\delta P}{P} \rangle \gtrsim 0.006e$.

VII. DISCUSSION

From Eq. (11), or (12) and (14), it can be seen that new terms contribute to the nonlinear polarization, so that critical intensity should decrease. This effect should be small and was not noticed in the plane-wave case. For other cases, in order to obtain a pattern, we need the value of the peak intensity, $|A_{\rm in0}|^2$, to be greater than the value for plane waves, which can be easily understood if we notice that $A_{\rm in}$ decays with ρ.

We considered the small effect of longitudinal fields in a widely studied model. We have found that the inclusion

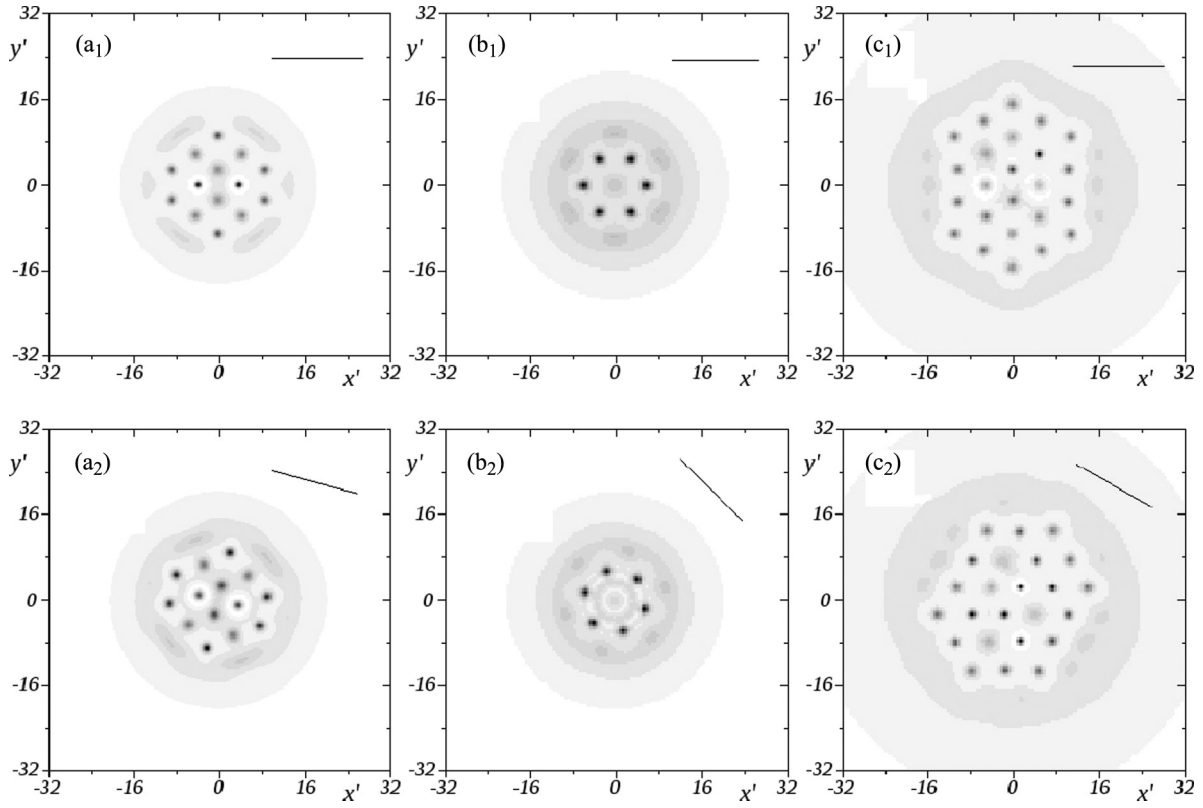

FIG. 4. Numerical integration results for different values of ρ_0'. In (a_1) and (a_2), $\rho_0' = 15$ and $K_N = 10^{-6}$. In all other cases, $K_N = 10^{-7}$, and 1/4 of the total area is shown. In (b_1) and (b_2) $\rho_0' = 28$. In (c_1) and (c_2) $\rho_0' = 60$. Polarization angles are as follows: for (a_1), (b_1), and (c_1) $\varphi = 0°$; in (a_2) $\varphi = 15°$; in (b_2) $\varphi = 45°$; in (c_2) $\varphi = 30°$. Pattern angles closely match polarization angles, except in (b_2), where the pattern orientates perpendicular to polarization direction.

of terms usualy neglected in the Lugiato-Lefever equation may have measurable consequences for transversely bounded beams. If there is no noise or if the noise is isotropic, pattern orientation is determined by field polarization. For anisotropic noise, pattern orientation is not determined but rather influenced by field polarization, even for relatively high noise. It would be interesting to study more realistic noise functions. Also, it would be interesting to study other input beams such as higher-order super-Gaussian beams, or top-hat beams, which provide a flat intensity region but have a very steep change in beam profile, and thus greater longitudinal fields.

There are many interesting phenomena related to beam propagation in Kerr media with or without cavities, like beam focusing [20], soliton formation [21], and light bullets [22]. Different possible applications have been proposed for Kerr-like materials, such as optical signal processing [23], all optical logical operators [24,25], cavities [26], and microcavities [27] used as switches and optical memories, and layers used as pulse shapers [28]. Modifications of NLSE accounting for different effects, like ultrashort temporal pulses or inhomogeneous media, have already been derived. However, longitudinal fields have been usually neglected in the analysis, even where widths are much smaller than the ones presented here, and thus greater longitudinal field effects should be expected. The results presented here should stimulate a closer look at orientation effects on those systems.

VIII. CONCLUSIONS

We have derived an equation for electromagnetic wave propagation in Kerr media. Transversely bounded fields and longitudinal fields have been taken into account. A mean-field equation describing field evolution in a cavity filled with such material was also derived. This equation was used to numerically integrate pattern forming situations in the cavity. An estimate of typical values for which these effects should be noticeable was presented.

For plane incident fields, taking into account longitudinal fields and other small terms did not generate any noticeable difference. For broad waist Gaussian beams, we found that critical intensity, pattern shape, and periodicity coincide with the already predicted values for incident plane waves. For smaller waists, the same patterns are formed, but their orientation can be controlled by the direction of electric-field polarization. Thus longitudinal fields, although small, may have measurable effects in nonlinear media. For very small beams, or for intensity greater that the critical values, we may find patterns with defects. The inclusion of noise in our analysis makes the orientation effect weaker, although some orientation effect prevails for typical values of noise intensity in, for example, low linewidth lasers.

In summary, the longitudinal component of the field can break rotational symmetry of the system, and broken symmetry is manifested in the orientation of the resulting patterns.

ACKNOWLEDGMENTS

D.M. wants to thank Miguel Hoyuelos for useful suggestions. This work was partially supported by Consejo Nacional de Investigaciones Científicas y Técnicas (CONICET, Argentina, PIP 0041 2010-2012). Part of this work was completed at INIFTA (UNLP-CONICET), through the "Beca postdoctoral Premio Fundacin Bunge y Born" fellowship granted to D.M.

APPENDIX A: OBTAINING AN EQUATION VALID TO ORDER α^4

The procedure for finding evolution equations is as usual. Starting from Eq. (4), we decompose each term into a fast oscillating wave and a slowly varying envelope. Then each slowly varying term and its derivative is expressed as a power series in α.

Under SVEA, we may write

$$-\mu_0\partial_t^2\vec{P}_L \simeq \left(k_0^2\vec{\mathcal{E}} + 2ik_0k'\frac{\partial\vec{\mathcal{E}}}{\partial t} + [-k'^2 - k_0k'']\frac{\partial^2\vec{\mathcal{E}}}{\partial t^2}\right) \times e^{i(k_0z-\omega_0t)} + \text{c.c.} \tag{A1}$$

Time derivatives of nonlinear polarization can be written in a similar way:

$$\mu_0\partial_t^2\vec{P}_{NL} = \vec{\mathcal{I}}e^{i(k_0z-\omega_0t)} + \text{c.c.}, \tag{A2}$$

$$\mathcal{I}_x = -\omega_0^2\mu_0\mathcal{P}_{NL,x} + i\left[2\left(\partial_{\omega_1}k^2_{(3)}|_0\right)|\mathcal{E}_x^2|\partial_t\mathcal{E}_x + \left(\partial_{\omega_3}k^2_{(3)}|_0\right)\mathcal{E}_x^2\partial_t\overline{\mathcal{E}_x}\right] + \cdots. \tag{A3}$$

Similar results are found for I_z after exchanging $x \leftrightarrow z$. They can be obtained from (8) and (A2).

Following the multiple scales analysis, the derivative of a quantity Q over a variable q can be written as

$$\frac{\partial Q}{\partial q} = \left(\frac{\partial}{\partial q_0} + \alpha\frac{\partial}{\partial q_1} + \alpha^2\frac{\partial}{\partial q_2} + \cdots\right)(Q^{(0)} + \alpha Q^{(1)} + \cdots), \tag{A4}$$

Derivation of Eqs. (9) and (10) can be done writing each term of Eqs. (4) and (5) as in the right side of Eq. (A4), finding expressions for each power of α. These expressions are solved and grouped again, like in the left-hand side of (A4). Equation (4) has already been worked this way up to order α^2, for instance, in [15]. Here we extend the results to order α^4 in a straightforward way, and then eliminate the ∂_{Z1} and ∂_{T1} derivatives.

At odds with other works, here we also consider Gauss equation (5). At order α, we get $\partial_{X_1}\mathcal{E}_x^{(0)} + ik_0\mathcal{E}_z^{(1)} = 0$. At order α^2, it reads $\partial_{X_2}\mathcal{E}_x^{(0)} + \partial_{X_1}\mathcal{E}_x^{(1)} + ik_0\mathcal{E}_z^{(2)} = 0$. This means that we can eliminate $\nabla\cdot\vec{E}$ components in (9). These equations also allow us to get rid of $\mathcal{E}_z$, since we may replace $\mathcal{E}_z$ by $\frac{i}{k_0}\partial_x\mathcal{E}_x + [O]^{(3)}$, where $[O]^{(3)}$ is of order α^3 or higher, and, if we apply operations of order α^2, like $\partial_x\partial_x$ or ∂_t, it does not bring any new term up to order α^4. At order α^4, we may write

$$[\partial_x\nabla\cdot(\vec{\mathcal{E}}e^{i(k_0z-\omega_0t)})]^{(4)} = -\frac{1}{\tilde{\varepsilon}_r(\omega_0)\varepsilon_0}\left(\partial^2_{X_1}[\mathcal{P}_{NL,x}]^{(2)} + ik_0\partial_{X_1}[\mathcal{P}_{NL,z}]^{(3)}\right). \tag{A5}$$

All these derivatives can be calculated using the definition of the nonlinear polarization (7).

APPENDIX B: COORDINATE TRANSFORMATION

Derivation of Eq. (11) is rather straightforward. The following step is to write it in a useful form: we need to eliminate derivatives over t and z in favor of derivatives over ξ and τ. Then we need to get rid of small terms containing ∂_ξ. We should recall that Eq. (9) can be rewritten as

$$[\partial_\xi\mathcal{E}_x]^{(2)} = \frac{i}{2k_0}[\nabla_\perp^2\mathcal{E}_x]^{(2)} + \frac{i}{2k_0}\omega_0^2\mu_0[\mathcal{P}_{NL,x}]^{(2)} + [O]^{(3)}, \tag{B1}$$

where $[O]^{(3)}$ are slowly varying terms of order α^3 or higher. Now if we are interested in calculating terms like $[\partial_x\partial_x\partial_\xi\mathcal{E}_x]^{(4)}$, since all considered terms are slowly dependent on x, $|\partial_x F| \leqslant \partial_{X1}F| \lesssim |\alpha F|$; thus $\partial_x\partial_x\partial_\xi O$ is of order $\alpha^{(5)}$ or higher and can be safely neglected. Similar results hold for $[\partial_t\partial_\xi\mathcal{E}_x]^{(4)}$.

Using this property repeatedly, we get (11), where

$$N_N = \frac{3\tilde{\chi}^{(3)}}{2\tilde{\varepsilon}_r(\omega_0)k_0}\{k^2[|\mathcal{E}_x|^2\mathcal{E}_x] + [(A_E+B_E)\mathcal{E}_x^2\partial_{xx}\bar{\mathcal{E}}_x + (A_E+B_E)|\mathcal{E}_x|^2\partial_{xx}\mathcal{E}_x + (4A_E+3B_E)\partial_x\mathcal{E}_x\partial_x\bar{\mathcal{E}}_x\mathcal{E}_x + (\partial_x\mathcal{E}_x)^2\bar{\mathcal{E}}_x]\}, \tag{B2}$$

$$N_T = \frac{3i}{2k_0}[2\partial_{\omega_1}k^{(3)2}\partial_t\mathcal{E}_x|\mathcal{E}_x^2| + \partial_{\omega_3}k^{(3)2}\mathcal{E}_x^2\partial_t\overline{\mathcal{E}_x}], \tag{B3}$$

and

$$N_L = \frac{-ik'}{2k_0^2}\partial_\tau\left(\nabla_\perp^2\mathcal{E}_x + \frac{3k_0^2\tilde{\chi}^{(3)}}{\tilde{\varepsilon}_r(\omega_0)}|\mathcal{E}_x|^2\mathcal{E}_x\right) - \frac{1}{2k_0}\Bigg\{\nabla_\perp^2\nabla_\perp^2\mathcal{E}_x/4k^2 + \frac{3\tilde{\chi}^{(3)}}{4k_0^2}\nabla_\perp^2(|\mathcal{E}_x|^2\mathcal{E}_x) + \frac{3\tilde{\chi}^{(3)}}{2\tilde{\varepsilon}_r(\omega_0)}(2|\mathcal{E}_x|^2\nabla_\perp^2\mathcal{E}_x - \mathcal{E}_x^2\nabla_\perp^2\bar{\mathcal{E}_x}) - k_0^2|\mathcal{E}_x|^4[2\tilde{\chi}^{(3)}/\tilde{\varepsilon}_r(\omega_0) - \overline{\tilde{\chi}^{(3)}/\tilde{\varepsilon}_r(\omega_0)}]\mathcal{E}_x\Bigg\}.$$

[1] L. A. Lugiato, M. Brambilla, and A. Gatti, Adv. At. Mol. Opt. Phys. **40**, 229 (1999).

[2] A. J. Scroggie, W. J. Firth, G. S. McDonald, M. Tlidi, R. Lefever, and L. A. Lugiato, Chaos Solitions Fractals **4**, 1323 (1994).

[3] L. A. Lugiato and R. Lefever, Phys. Rev. Lett. **58**, 2209 (1987).

[4] R. W. Boyd, *Nonlinear Optics*, 3rd ed. (Academic, New York, 2007).

[5] M. Hoyuelos, P. Colet, M. San Miguel, and D. Walgraef, Phys. Rev. E **58**, 2992 (1998).

[6] P. Jakobsen and J. V. Moloney, Physica D **241**, 1603 (2012); B. A. Malomed, K. Marinov, D. I. Pushkarov, and A. Shivarova, Phys. Rev. A **64**, 023814 (2001).

[7] G. Fibich and B. Ilan, Physica D **157**, 112 (2001).

[8] C. G. Chen, P. T. Koukola, J. Ferrera, R. K. Heilmann, and M. L. Schattenburg, J. Opt. Soc. Am. A **19**, 404 (2002).
[9] M. Lax, W. H. Luisell, and W. B. McKnight, Phys. Rev. A **11**, 1365 (1975).
[10] G. P. Agrawal and D. N. Pattamayak, J. Opt. Soc. Am. **69**, 575 (1979).
[11] G. P. Agrawal and M. Lax, Phys. Rev. A **27**, 1693 (1983).
[12] Y. I. Salamin, Appl. Phys. B **86**, 319 (2007).
[13] A. E. Siegman, *Lasers* (University Science Books, Mill Valley, CA, 1986).
[14] J. V. Moloney and A. C. Newell, *Nonlinear Optics* (Westview Press, Boulder, CO, 2003).
[15] P. Tassin, G. Van der Sande, I. Veretennicoff, M. Tlidi, and P. Kockaert, Proc. SPIE **5955**, 59550X (2005).
[16] M. Scalora, M. S. Syrchin, N. Akozbek, E. Y. Poliakov, G. D'Aguanno, N. Mattiucci, M. J. Bloemer, and A. M. Zheltikov, Phys. Rev. Lett. **95**, 013902 (2005).
[17] Numerical integrations were performed with the following parameters: time discretization was 7×10^{-3}, spatial discretization was $\Delta x = 1/2$, except for $\rho_0' = 15$, where $\Delta x = 1/4$. Integration domain consists in a 256×256 points square, except for subsection noise, where a grid of 512×512 was considered periodic boundary conditions and also zero-field boundary conditions were used, without noticeable differences in the central area. Temporal evolution was calculated by means of a fourth-order Runge-Kutta method. Fast Fourier transform was used for calculating derivatives. Initial conditions consisted of a circularly symmetric function that corresponds to the solution of the original equation (i.e., $\hat{O} = 0$) for a lower intensity ($A_{\text{in}} = 1$ instead of 1.035).
[18] F. Papoff, G. D. D'Alessandro, G.-L. Oppo, and W. J. Firth, Phys. Rev. A **48**, 634 (1993).
[19] J.-S. Huang, H. Su, X. He, C. Lei, R. Zendejaz, R. Agarwal, M. Lomeli, J. Ye, H. Chin, and H. Kim, in *Photonics Conference (PHO), 2011 IEEE* (Arlington, VA, 2011), pp. 212–213; J. S. Huang, H. Lu, and H. Su, in *21st Annual Meeting of the LEOS: IEEE Lasers and Electro-Optics Society, 2008* (Newport Beach, CA, 2008), pp. 894–895; J. Geng, S. Staines, Z. Wang, J. Zong, M. Blake, and S. Jiang, IEEE Photonics Technol. Lett. **18**, 1813 (2006).
[20] J. H. Marburger, Prog. Quantum Electron. **4**, 35 (1975).
[21] Z. Chen, M. Segev, and D. N. Christodoulides, Rep. Prog. Phys. **75**, 086401 (2012).
[22] M. Matuszewski, M. Trippenbach, B. A. Malomed, E. Infeld, and A. A. Skorupski, Phys. Rev. E **70**, 016603 (2004); D. Mihalache, D. Mazilu, B. A. Malomed, F. Lederer, L.-C. Crasovan, Y. V. Kartashov, and L. Torner, *ibid.* **74**, 047601 (2006); G. Fibich and B. Ilan, Opt. Lett. **29**, 887 (2004).
[23] J. P. Burger, S. Dubovitsky, and W. H. Steier, Opt. Commun. **212**, 251 (2002).
[24] A. Jacobo, D. Gomila, M. A. Matías, and P. Colet, New J. Phys. **14**, 013040 (2012).
[25] T. Fujisawa and M. Koshiba, J. Opt. Soc. Am. B **23**, 684 (2006).
[26] M. A. Antón, O. G. Calderón, S. Melle, I. Gonzalo, and F. Carreo, Opt. Commun. **268**, 146 (2006); Z. H. Xiao and K. Kim, *ibid.* **283**, 2178 (2010).
[27] L. Gelens, S. Beri, G. Van der Sande, G. Mezosi, M. Sorel, J. Danckaert, and G. Verschaffelt, Phys. Rev. Lett. **102**, 193904 (2009).
[28] J. Wei, M. Xiao, and F. Zhang, Appl. Phys. Lett. **89**, 223126 (2006).